

Molecular Structure of a Mixed-Valence 1,1'-Biruthenocene Derivative, Iodobiruthenocenium(II,IV) Tetrafluoroborate

Masanobu Watanabe,^{*1a} Izumi Motoyama,^{1a} Mamoru Shimoi,^{1b} and Toschitake Iwamoto^{1b}

Department of Chemistry, Faculty of Engineering, Kanagawa University, Rokkakubashi, Yokohama 221, Japan, and College of Arts and Sciences, The University of Tokyo, Komaba, Meguro, Tokyo 153, Japan

Received October 14, 1993*

The crystal structure of iodo-1,1'-biruthenocenium(II,IV) tetrafluoroborate, $[\text{Ru}^{\text{II}}\text{Cp}(\text{H}_4\text{C}_5\text{C}_5\text{H}_4)\text{CpRu}^{\text{IV}}]^+\text{BF}_4^-$, which is prepared by oxidation of 1,1'-biruthenocene, R_cR_c, with the iodoruthenocenium(IV)⁺BF₄⁻ salt, has been determined by X-ray analysis. It crystallizes in the monoclinic space group $P2_1/n$ with $a = 25.078(12)$ Å, $b = 10.599(12)$ Å, $c = 7.652(8)$ Å, $\beta = 95.17(8)^\circ$, $V = 2026(3)$ Å³, and $Z = 4$, and the final R obtained was 0.075. The cation has a trans conformation. The cyclopentadienyl rings in the $[\text{Cp}(\text{C}_5\text{H}_4)\text{Ru}]^+$ moiety are slanted largely due to the bond formation of the I–Ru^{IV} bond (2.717(2) Å). The dihedral angle between the Cp ring and fulvenide ligand is found to be 42.40°.

Introduction

Recently, we reported on electron-exchange reactions of mixed-valence halobiruthenocenium(II,IV)⁺Y⁻, $[\text{RcRcX}]^+\text{Y}^-$, halodialkylbiruthenocenium⁺Y⁻, $[\text{RcRcR}_2\text{X}]^+\text{Y}^-$ (R = Et, Pr; X = Cl, Br, I; Y = I₃, PF₆), and related salts in acetone and other solvents, by means of ¹H- and ¹³C-NMR spectroscopy.^{2–5} In these studies, NMR signals due to trapped-valence states of Ru^{II} and Ru^{IV} observed below ca. 200 K moved together and eventually coalesced into signals due to the averaged-valence state over Ru^{II} and Ru^{IV} on the NMR time scale, as the temperature increased. The E_a values of the electron-exchange reactions increase in the order $[\text{RcRcPr}_2\text{X}]^+ > [\text{RcRcEt}_2\text{X}]^+ > [\text{RcRcX}]^+$.

Although a large number of structural studies of mixed-valence biferrocenium salts have been reported,^{6–10} no structural studies on mixed-valence biruthenocenium salts have been reported. In this paper, the crystal structure of $[\text{Ru}^{\text{II}}\text{Cp}(\text{H}_4\text{C}_5\text{C}_5\text{H}_4)\text{CpRu}^{\text{IV}}]^+\text{BF}_4^-$ (**1**) is discussed in comparison with that of neutral R_cR_c, which should afford better understanding of the chemistry of mixed-valence halobiruthenocenium(II,IV) salts.

Experimental Section

Syntheses. Salt **1** was prepared as follows: R_cR_c (100 mg, 0.22 mmol) dissolved in 50 cm³ of CH₂Cl₂ was added to a CH₂Cl₂ solution containing a stoichiometric amount of $[\text{RcHI}]^+\text{BF}_4^-$ (97.9 mg, 0.22 mmol). After

the mixture was stirred for 1 h, the solvent was evaporated. After removal of R_cH by extraction with benzene, **1** was obtained from the solution by recrystallization from a CH₂Cl₂–C₆H₁₂ mixture as deep purple crystals (125 mg; yield 84%). Single crystals suitable for X-ray study were obtained from the CH₂Cl₂ solution of **1** by diffusion of hexane vapor at room temperature. Anal. Calcd for C₂₀H₁₈BF₄IRu₂: C, 35.63; H, 2.69. Found: 35.02; H, 2.44.

Physical Measurements. The ¹H-NMR spectra were recorded with a JEOL FX-90Q Fourier transform NMR spectrometer at 89.59 MHz using TMS as a standard under the conditions reported previously in our papers.^{3–5} ¹³C-CP-MAS NMR spectra were recorded under the conditions similar to those applied in our previous report.¹¹

X-ray Crystallography. A deep-purple plate having approximate dimensions of 0.3 × 0.2 × 0.04 mm³ was selected. X-ray diffraction experiments were carried out on a Rigaku AFC-5 automated four-circle X-ray diffractometer with graphite-monochromatized Mo Kα (λ = 0.710 73 Å) radiation. The lattice parameters were determined by a least-squares calculation from 25 reflections. During the intensity collection, no decrease in the standard reflection intensities was observed; among 6764 independent reflections measured, 5434 were observed with $|F_o| > 3\sigma(F_o)$. Intensity data were collected over the range of 4° ≤ 2θ ≤ 60° using the ω–2θ scan mode with a scanning speed of 4° min⁻¹, and the range of indices was –35 ≤ h ≤ 35, 0 ≤ k ≤ 15, 0 ≤ l ≤ 11. The reflection data were corrected with Lorentz and polarization factors and for absorption¹² but not for extinction.

The structure of **1** was solved by heavy-atom methods. The positions of the ruthenium and iodine atoms were deduced from the Patterson map, and the other atoms (C, B, F) were located by successive Fourier syntheses. Their positional and thermal parameters were refined by block-diagonal least-squares methods. The thermal motions of the non-hydrogen atoms were refined anisotropically. Positions of hydrogen atoms were calculated using fixed positions ($d(\text{C–H}) = 1.08$ Å), applying thermal parameters 1.5 times the equivalent isotropic ones for the carbon atoms to which they were attached. The refinement converged to $R = 0.075$ and $R_w = 0.072$. The atomic-scattering factors for non-hydrogen atoms and hydrogen atoms were taken from refs 13 and 14, respectively. All calculations were carried out on a FACOM FMR60 computer at the Educational Computer Center of the University of Tokyo, using the

* Abstract published in *Advance ACS Abstracts*, May 1, 1994.

- (1) (a) Kanagawa University. (b) The University of Tokyo.
- (2) Watanabe, M.; Sano, H.; Motoyama, I. *Chem. Lett.* **1990**, 1667. Watanabe, M.; Kawata, S.; Sano, H.; Motoyama, I. *J. Organomet. Chem.* **1990**, 399, 301.
- (3) Watanabe, M.; Iwamoto, T.; Sano, H.; Kubo, A.; Motoyama, I. *J. Organomet. Chem.* **1992**, 441, 309. Watanabe, M.; Iwamoto, T.; Kawata, S.; Kubo, A.; Sano, H.; Motoyama, I. *Inorg. Chem.* **1992**, 31, 177.
- (4) Watanabe, M.; Iwamoto, T.; Sano, H.; Motoyama, I. *J. Coord. Chem.* **1992**, 26, 223. Watanabe, M.; Iwamoto, T.; Sano, H.; Motoyama, I. *Inorg. Chem.* **1993**, 32, 5223.
- (5) Watanabe, M.; Iwamoto, T.; Sano, H.; Motoyama, I. *J. Organomet. Chem.* **1992**, 31, 177. Watanabe, M.; Iwamoto, T.; Sano, H.; Motoyama, I. *J. Organomet. Chem.* **1992**, 31, 177.
- (6) Nakashima, S.; Konno, K.; Sano, H. *Hyperfine Interact.* **1991**, 68, 205.
- (7) Konno, K.; Sano, H. *Bull. Chem. Soc. Jpn.* **1988**, 61, 1455.
- (8) Dong, T.-Y.; Schei, C. C.; Hwang, M. Y.; Lee, T.-Y. *J. Organomet. Chem.* **1991**, 410, C39.
- (9) Dong, T.-Y.; Hendrickson, D. N.; Iwai, K.; Cohn, M. J.; Geib, S. J.; Rheingold, A. L.; Sano, H.; Motoyama, I.; Nakashima, S. *J. Am. Chem. Soc.* **1985**, 107, 7996.
- (10) Dong, T.-Y.; Hwang, M.-Y.; Schei, C.-C.; Peng, S.-M.; Yeh, S.-K. *J. Organomet. Chem.* **1989**, 369, C33. Dong, T.-Y.; Hwang, M.-Y.; Hsu, T.-L.; Schei, C.-C.; Yeh, S.-K. *Inorg. Chem.* **1990**, 29, 80.

- (11) Watanabe, M.; Masuda, Y.; Motoyama, I.; Sano, H. *Bull. Chem. Soc. Jpn.* **1988**, 61, 827.
- (12) North, A. T. C.; Phillips, D. C.; Mathews, F. S. *Acta Crystallogr.* **1988**, A24, 351.
- (13) *International Tables for X-ray Crystallography*; Kynoch: Birmingham, England, 1974; Vol. IV, Table 2.2A (pp 72–98), Table 2.3.1.1 (pp 149–150).
- (14) Stewart, R. F.; Davidson, E. R.; Simpson, W. T. *J. Chem. Phys.* **1965**, 42, 3175–3187.

Table 1. Crystal and Intensity Collection Data for **1**

formula	C ₂₀ H ₁₈ BF ₄ IRu ₂	Z	4
fw	674.211	T/°C	17
space group	P2 ₁ /n (variant of No. 14)	λ/Å	0.710 73
a/Å	25.078(12)	μ/cm ⁻¹	30.4
b/Å	10.599(12)	no. of reflns measd	6764
c/Å	7.652(8)	no. of obsd. reflns, F _o > 3σ F _o	5434
β/deg	95.17(8)	R ^a	0.075
V/Å ³	2026(3)	R _w ^b	0.072

^a $R = \sum ||F_o| - |F_c|| / \sum |F_o|$. ^b $R_w = (\sum w(|F_o| - |F_c|)^2 / \sum w(|F_o|^2))^{1/2}$. $w = 0.25 + 0.0375|F_o|$ for $|F_o| < 20.0$, $w = 1.0$ for $20.0 \leq |F_o| \leq 100.0$, and $w = 10000/(3|F_o|^2 - 20000)$ for $100 < |F_o|$.

Table 2. Atomic Coordinates ($\times 10^4$) and Isotropic Temperature Factors ($\text{\AA}^2 \times 10^2$)

atom	x	y	z	B _{eq} ^a
I(1)	1535.7(2)	5546.7(6)	9079.0(7)	3.5
Ru(1)	1858.7(3)	4280.2(7)	6272.6(8)	2.8
Ru(2)	300.3(3)	7534.6(6)	3621.8(8)	2.7
C(1)	2088(6)	2278(11)	6601(19)	6.0
C(2)	2109(5)	2824(13)	8246(17)	5.6
C(3)	2516(5)	3753(13)	8313(14)	5.2
C(4)	2728(4)	3769(13)	6683(16)	5.2
C(5)	2453(5)	2891(13)	5637(16)	5.7
C(6)	1189(3)	5795(8)	4982(9)	2.8
C(7)	1710(4)	5962(9)	4399(11)	3.2
C(8)	1833(4)	4812(10)	3548(11)	3.8
C(9)	1429(4)	3898(10)	3776(12)	4.0
C(10)	1054(3)	4469(8)	4783(11)	3.2
C(11)	861(3)	6750(8)	5647(11)	2.9
C(12)	956(4)	8085(9)	5497(13)	3.9
C(13)	492(5)	8715(11)	5949(14)	4.8
C(14)	104(5)	7838(11)	6332(12)	4.6
C(15)	326(4)	6597(9)	6152(11)	3.5
C(16)	143(7)	8750(12)	1345(15)	5.8
C(17)	505(6)	7857(14)	983(13)	5.9
C(18)	265(5)	6609(10)	1067(12)	4.2
C(19)	-261(5)	6807(12)	1494(13)	4.7
C(20)	-326(5)	8145(14)	1669(14)	5.6
B	640(5)	4553(13)	7165(17)	4.5
F(1)	6293(5)	4221(8)	8328(15)	9.4
F(2)	6389(4)	4742(12)	5528(13)	9.5
F(3)	7028(4)	3637(8)	7060(11)	7.0
F(4)	6885(4)	5663(8)	7657(12)	7.2

^a $B_{eq} = \frac{1}{3}(B_{11}a^2 + B_{22}b^2 + B_{33}c^2 + B_{13}ac \cos \beta)$; B_{ij} 's are defined by $\exp[-(h^2B_{11} + k^2B_{22} + l^2B_{33} + 2klB_{23} + 2hlB_{13} + 2hkB_{12})]$.

UNICS-III program.¹⁵ Crystallographic data for **1** and some of the experimental conditions for the X-ray structure analysis are listed in Table 1.

Results and Discussion

The final atomic coordinates and equivalent isotropic temperature factors ($B_{eq}/\text{\AA}^2$) of non-hydrogen atoms for **1** are shown in Table 2, and an ORTEP drawing of the [RcRcI]⁺ cation with the atom-numbering system is shown in Figure 1. As has been observed in all other structures of neutral R₂Cp₂,¹⁶ biferrocene,¹⁷ and mixed-valence biferrocenium salts,⁶⁻¹⁰ the two Cp rings are transoid to the fulvalene ligand (C₅H₄C₅H₄). The Ru(I)⋯Ru(2) distance is 5.464(4) Å, which shows no direct interaction between them. A striking feature of the salt is observed at the Ru(1) side. Iodine is coordinated to the Ru(1) atom; the Ru(1)–I distance (2.717(2) Å) is shorter than the Ru^{IV}–I bond in the [RcHI]⁺ cation (2.732(3) Å¹⁸) and comparable with the Ru–I bond in

Table 3. Interatomic Distances (Å) for **1**

Ru(1)–Ru(2)	5.464(4)	Ru(1)–I	2.717(2)
Ru(2)–I	5.398(5)	Ru(1)–C(1)	2.207(12)
Ru(1)–C(2)	2.211(13)	Ru(1)–C(3)	2.238(11)
Ru(1)–C(4)	2.240(11)	Ru(1)–C(5)	2.182(14)
Ru(1)–C(6)	2.464(8)	Ru(1)–C(7)	2.297(9)
Ru(1)–C(8)	2.155(9)	Ru(1)–C(9)	2.146(9)
Ru(1)–C(10)	2.235(9)	Ru(2)–C(11)	2.163(8)
Ru(2)–C(12)	2.163(10)	Ru(2)–C(13)	2.194(11)
Ru(2)–C(14)	2.198(10)	Ru(2)–C(15)	2.172(9)
Ru(2)–C(16)	2.174(12)	Ru(2)–C(17)	2.155(11)
Ru(2)–C(18)	2.182(10)	Ru(2)–C(19)	2.195(11)
Ru(2)–C(20)	2.167(12)	C(1)–C(2)	1.38(2)
C(2)–C(3)	1.42(2)	C(3)–C(4)	1.40(2)
C(4)–C(5)	1.37(2)	C(5)–C(1)	1.39(2)
C(6)–C(7)	1.43(1)	C(7)–C(8)	1.43(1)
C(8)–C(9)	1.42(2)	C(9)–C(10)	1.40(1)
C(10)–C(6)	1.45(1)	C(11)–C(12)	1.44(1)
C(12)–C(13)	1.41(2)	C(13)–C(14)	1.40(2)
C(14)–C(15)	1.44(2)	C(15)–C(11)	1.44(1)
C(16)–C(17)	1.36(2)	C(17)–C(18)	1.46(2)
C(18)–C(19)	1.40(2)	C(19)–C(20)	1.44(2)
C(20)–C(16)	1.38(2)	C(6)–C(11)	1.43(1)
B–F(1)	1.345(18)	B–F(2)	1.365(16)
B–F(3)	1.383(16)	B–F(4)	1.364(16)

Table 4. Bond Angles (deg) for **1**

C(1)–C(2)–C(3)	107.1(12)
C(2)–C(3)–C(4)	107.8(11)
C(3)–C(4)–C(5)	107.6(11)
C(4)–C(5)–C(1)	109.1(11)
C(5)–C(1)–C(2)	108.3(12)
C(6)–C(7)–C(8)	106.1(8)
C(7)–C(8)–C(9)	109.9(9)
C(8)–C(9)–C(10)	107.0(9)
C(9)–C(10)–C(6)	108.3(8)
C(10)–C(6)–C(7)	107.4(7)
C(7)–C(6)–C(11)	126.6(8)
C(10)–C(6)–C(11)	126.0(8)
C(6)–C(11)–C(12)	124.3(8)
C(6)–C(11)–C(15)	126.7(8)
C(12)–C(11)–C(15)	107.3(8)
C(11)–C(12)–C(13)	107.4(9)
C(12)–C(13)–C(14)	110.0(10)
C(13)–C(14)–C(15)	107.7(10)
C(14)–C(15)–C(11)	107.5(9)
C(16)–C(17)–C(18)	109.7(12)
C(17)–C(18)–C(19)	106.0(11)
C(18)–C(19)–C(20)	106.6(11)
C(19)–C(20)–C(16)	109.6(12)
C(20)–C(16)–C(17)	108.1(12)
F(1)–B–F(2)	112.0(12)
F(1)–B–F(3)	110.8(11)
F(1)–B–F(4)	110.2(11)
F(2)–B–F(3)	108.5(11)
F(2)–B–F(4)	106.6(11)
F(3)–B–F(4)	108.6(11)

Ru(CO)₄I₂ (2.719(7) Å¹⁹). The distance between Ru(2) and I (5.398(5) Å) shows no bond formation between Ru(2) and I. The oxidation states of Ru(1) and Ru(2) can be assigned as Ru^{IV} and Ru^{II}, respectively; i.e., the cation is formulated as [Ru^{II}Cp-(C₅H₄C₅H₄)CpRu^{IV}I]⁺ in the solid. The results obtained above correspond well to those of the ¹³C-CP-MAS NMR spectroscopic study of [RcRcI]⁺I₃⁻. Two kinds of carbon atoms in the Cp rings (77.4 ppm ([Ru^{II}Cp(C₅H₄)] moiety) and 92.9 ppm ([C₅H₄–CpRu^{IV}]⁺ moiety) are observed at room temperature.³

It is important to compare the molecular structure parameters of the cation with those previously reported for R₂Cp²⁰ and R₂Cp¹⁶ and [RcHI]⁺I₃⁻.¹⁸ The five-membered Cp rings of Ru^{II} (C(1)–C(5)) and Ru^{IV} (C(16)–C(20)) form regular pentagons. Average Cp ring C–C lengths of Ru^{II} and Ru^{IV} are 1.39(2) and 1.41(4)

(15) Sakurai, T.; Kobayashi, M. *Rikagaku Kenkyusho Hokoku* **1979**, 55, 69.

(16) Levendis, D. C.; Boeyens, J. C. A.; Neuse, E. W. *J. Crystallogr. Spectrosc. Res.* **1982**, 12, 493.

(17) Macdonald, A. C.; Trotter, J. *Acta Crystallogr.* **1964**, 17, 872. Boeyens, J. C. A.; Neuse, E. W.; Levendis, D. C. *S. Afr. J. Chem.* **1982**, 35, 57.

(18) Sohn, Y. S.; Schlueter, A. W.; Hendrickson, D. N.; Gray, H. B. *Inorg. Chem.* **1974**, 13, 301.

(19) Dahl, L. F.; Wampler, D. L. *Acta Crystallogr.* **1962**, 15, 946.

(20) Hardgrove, G. L.; Templeton, D. H. *Acta Crystallogr.* **1959**, 12, 28.

(21) Geib, S. J.; Rheingold, A. L.; Dong, T.-Y.; Hendrickson, D. N. *J. Organomet. Chem.* **1986**, 312, 241.

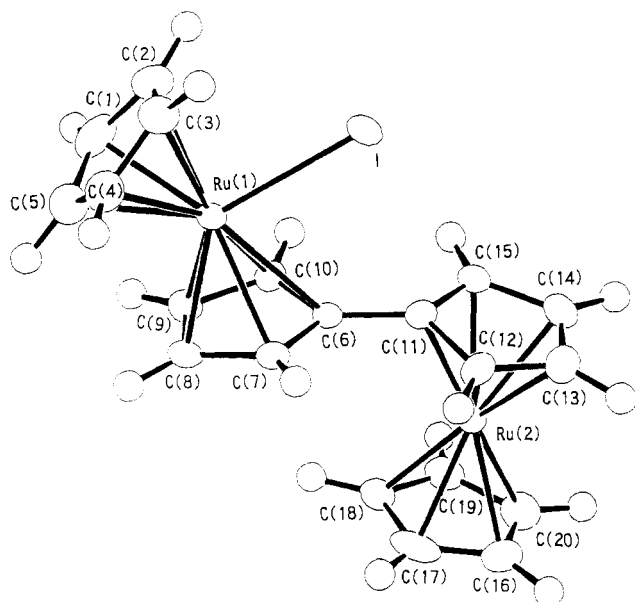


Figure 1. ORTEP drawing of $[\text{Ru}^{\text{II}}\text{Cp}(\text{C}_5\text{H}_4\text{H}_4\text{C}_5)\text{CpRu}^{\text{IV}}]^+$ cation with the numbering scheme of the atoms.

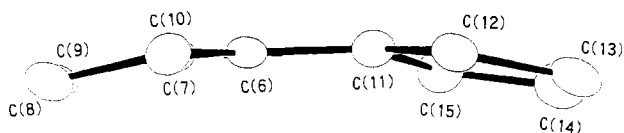


Figure 2. ORTEP drawing of conjugated fulvalene ligand with the numbering scheme of the atoms.

Table 5. Dihedral Angles between Planes (deg)

plane	plane		
	C(6)–C(10)	C(11)–C(15)	C(11)–C(15)
C(1)–C(5)	42.40	61.44	59.72
C(6)–C(10)		19.35	17.34
C(11)–C(15)			5.19

Å, respectively, and these values are comparable to those obtained for R_cH (1.43(3) Å), R_cR_c (1.42(1) Å), and [R_cH]⁺I₃[−] (1.41(3) Å).

The difference of oxidation states is reflected in the Ru–C(Cp) bond lengths. The average Ru(1)–C(Cp) bond length (2.216(22) Å), which is slightly longer than the value of the [R_cH]⁺ cation (2.197(12) Å),¹⁸ is significantly longer than the Ru(2)–C(Cp) bond (2.175(10) Å). The average distance from Ru(1) to the Cp rings (1.879(7) Å), which is longer than that for the [R_cH]⁺ cation (1.84 Å), is also longer than the value for Ru(2)–Cp ring (1.812(3) Å). Thus, expansion of the metal–carbon bond lengths is observed with an increase in the Ru oxidation state (II → IV). Such expansion in bond lengths on the Ru^{IV} side may be due to the removal of bonding electrons (*e*_{2g}). These results are comparable with those obtained for mixed-valence biferrrocenium salts (in the case of the biferrrocenium(II,III)⁺FeBr₄[−] salt, the distance between two Cp rings on the Fe^{III} side (3.38(2) Å) is significantly longer than that found on the Fe^{II} side (3.30(2) Å).¹⁹ The most interestingly results in the structure analysis are an extraordinarily large dihedral angle observed in the [Ru^{II}–Cp(C₅H₄)I]⁺ moiety and the nonplanarity of the fulvenide ligand C(6)–C(15), as shown in Figure 2. Although the Cp rings of neutral R_cR_c, biferrrocene, and mixed-valence biferrrocenium salts are essentially parallel to the fulvenide ligand, the dihedral angle of the Cp rings of Ru(1) is found to be 42.4° (the angle is 5.19° in the Ru(2) side, as shown in Table 5). This value corresponds well to that of the iodo[2]ferrocenophanium triiodide salt (41°)

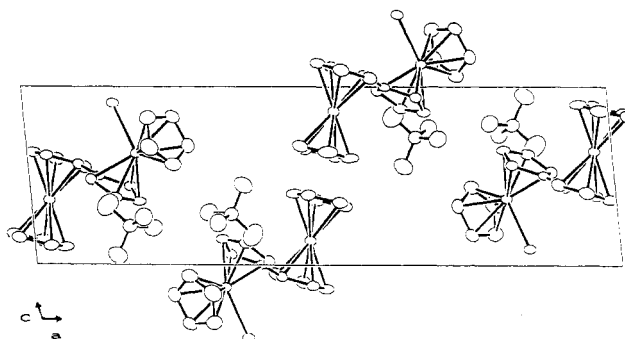


Figure 3. Projection of the unit cell of **1** along the *b*-axis.

with an Fe–I bond,²² and the value is larger than that of [R_cH]⁺I₃[−] (the angle is 32.2°¹⁸), [1.1]ruthenocenophanium(2+)(BF₄[−])₂ (28°, in which the Ru^{III}–Ru^{III} bond = 2.951(1) Å²³), osmocenium(2+)(PF₆[−])₂ (35.5°, in which the Os^{III}–Os^{III} bond = 3.038(0) Å²⁴), and [(η⁵,η⁵-C₅Me₄(CH₂)₃C₅Me₄)Fe^{IV}(NCCH₃)]²⁺·(PF₆[−])₂ (34.5°, the Fe^{IV}–NCCH₃ bond = 1.916(6) Å²⁵).

As shown in Figure 2, the fulvenide system C(6)–C(15) is not planar in contrast to the planar fulvenide (C₅H₄C₅H₄) systems for R_cR_c¹⁶ and mixed-valence biferrrocenium salts;^{6–10,19} the dihedral angle between the plane C(6)–C(10) and C(11)–C(15) is found to be 19.35°. Moreover, the dihedral angle between the plane C(7)–C(6)–C(10) and C(7)–C(8)–C(9)–C(10) on the Ru^{IV} side is 11.60° (the corresponding angle between the plane C(12)–C(11)–C(15) and C(12)–C(13)–C(14)–C(15) on the Ru^{II} side is 1.21°). The bond length of Ru(1)–C(6) (2.464(8) Å) is much larger than the other Ru(1)–C bonds in the Cp ring (2.146(9)–2.297(9) Å); i.e., the C(6) atom is out of plane. The distances of I···C(6) and I···C(11) are found to be 3.188(8) and 3.253(9) Å, respectively. These values are less than the sum of van der Waals' radii of C and I (3.85 Å).²⁶ Thus the large dihedral angle of the Cp ring for Ru^{IV} (larger than [R_cH]⁺I₃[−] by 10.2°) and the anomalous nonplanar feature of the fulvenide ring could be caused by the repulsion between I and the C(6) and C(11) atoms.

A projection of the unit cell along the *b* axis is shown in Figure 3. The tetrahedral BF₄[−] anion shows large thermal motion (*B*_{eq} = 7.0–9.5 Å²). The average B–F distance of the anion is 1.364(16) Å, and the average F–B–F angle is 109.5(18)°; the values are similar to those reported for (ferrocenyldiphenylcarbenium(+))BF₄[−] salt.²⁷ The shortest distances between each F atom and C atom in the Cp ring are 3.338(14) Å for F(1)–C(9), 3.307(17) Å for F(2)–C(4), 3.326(16) Å for F(3)–C(2), and 3.364(14) Å for F(4)–C(3); i.e., the BF₄[−] anion is located closer to the higher positive charge of the [Cp(C₅H₄)–Ru^{IV}]⁺ moiety.

¹H-NMR Spectroscopic Studies. As indicated in the Introduction, the most interesting phenomenon of the mixed-valence halobiruthenocenium(II,IV) salts is observed in their ¹³C- and ¹H-NMR spectra in solution.^{2–5} As shown in Figure 4, ¹H-NMR spectra of **1** (concentration of 0.014 mol dm^{−3}) exhibit a remarkable temperature dependence. This is in contrast with the absence of temperature dependence of NMR spectra for neutral R_cR_c as in the same conditions of **1**. Six sharp peaks were observed at 183 K. The three peaks at lower field (δ = 6.41, 6.05, 5.80) can be assigned to Cp ring protons of the Ru^{IV} side, and the other three peaks (δ = 5.36, 5.21, 4.64), to those of the

(22) Watanabe, M.; Sato, K.; Motoyama, I.; Sano, H. *Chem. Lett.* **1983**, 1775.

(23) Mueller-Westerhoff, U. T.; Rheingold, A. L.; Swiegers, G. F. *Angew. Chem., Int. Ed. Engl.* **1992**, *31*, 1353.

(24) Droege, M. W.; Harman, W. D.; Taube, H. *Inorg. Chem.* **1987**, *26*, 1309.

(25) Ogino, H.; Tobita, H.; Habazaki, H.; Shimoi, M. *J. Chem. Soc., Chem. Commun.* **1989**, 828.

(26) Pauling, L. *The Nature of the Chemical Bond*, 3rd ed.; Cornell Univ. Press: Ithaca, NY, 1960.

(27) Behrens, U. *J. Organomet. Chem.* **1979**, *182*, 89.

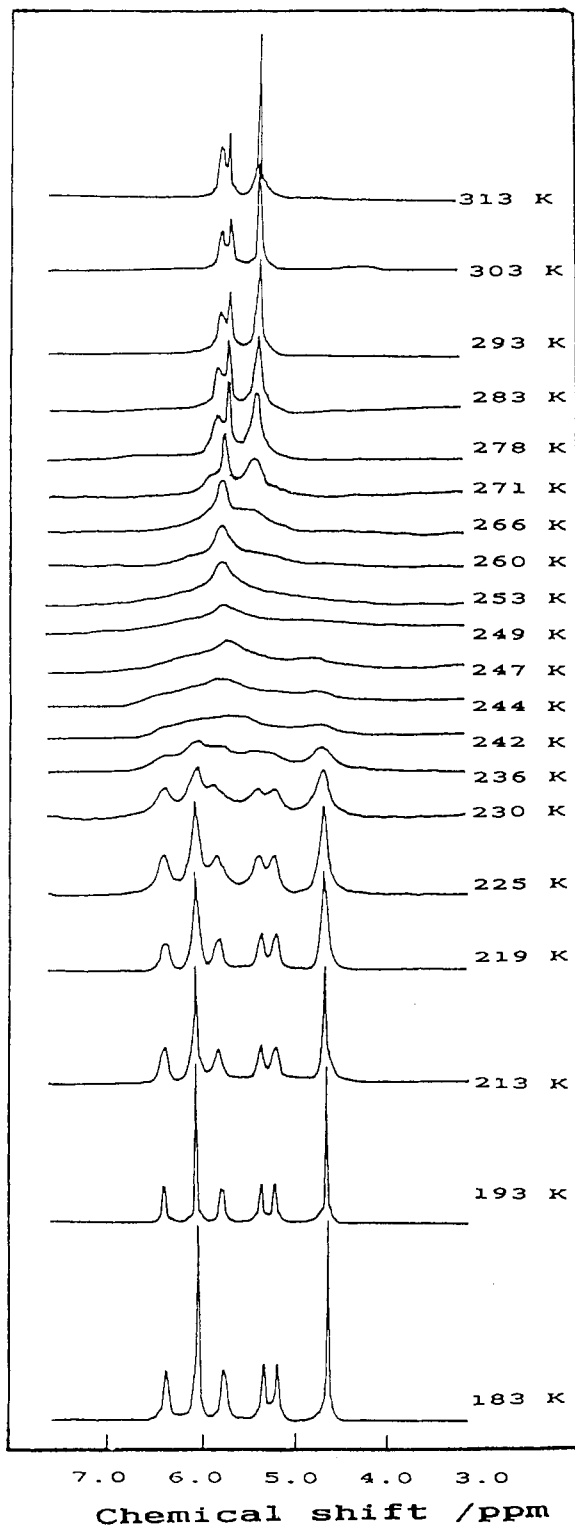


Figure 4. Temperature-dependent 90-MHz ^1H -NMR spectra of **1** in acetone- d_6 at indicated temperatures.

Ru^{II} side. Hence the formula of **1** in acetone at 183 K is given as $[\text{Ru}^{\text{II}}\text{Cp}(\text{C}_5\text{H}_4\text{C}_3\text{H}_4)\text{CpRu}^{\text{IV}}\text{I}]^+\text{BF}_4^-$ and the structure of the cation should remain intact in a trans conformation even in the

solution because of a higher steric hindrance of the Ru^{II} and Ru^{IV} atoms in the cis conformation. This conclusion was confirmed by the reported studies; i.e., the ^{13}C -CP-MAS NMR spectra of mixed-valence $[\text{RcRcX}]^+\text{Y}^-$ ($\text{X} = \text{I}, \text{Br}, \text{Cl}; \text{Y} = \text{PF}_6, \text{I}_3$) correspond well to the ^{13}C -NMR spectra in acetone at 183 K.³

Upon heating of the samples, these peaks were broadened, and the coalescence temperature, T_c , was about 248 ± 1 K, corresponding well to the value for $[\text{RcRcI}]^+\text{I}_3^-$. Above T_c , three sharp lines ($\delta = 5.72, 5.63, 5.33$) were observed at 313 K. On the basis of the results of the reported and present studies, it can be concluded that there occurs an electron-exchange reaction between Ru^{II} and Ru^{IV} .

To estimate the activation parameters for the migration, NMR spectral simulations were carried out by the reported method of calculation.^{3-5,28} From the results, the activation energy, E_a , and ΔG^\ddagger , ΔH^\ddagger , and ΔS^\ddagger values were estimated to be 37.1 ± 0.6 , 51.9 ± 0.4 , 34.6 ± 0.6 kJ mol $^{-1}$, and -58.1 ± 3.4 J K $^{-1}$ mol $^{-1}$, respectively, and the values correspond well to those of $[\text{RcRcI}]^+\text{I}_3^-$,^{3,5} i.e., there is no counterion effect on the electron-exchange reaction between Ru^{II} and Ru^{IV} in acetone.

Recently, diruthenocenylmethane (RcCH_2Rc , $\text{Ru}^{\text{II}}\text{Cp}(\text{C}_5\text{H}_4\text{CH}_2\text{C}_3\text{H}_4)\text{CpRu}^{\text{II}}$) was first prepared, and oxidation of RcCH_2Rc with I_2 gave a mixed-valence salt formulated as $[\text{Ru}^{\text{II}}\text{Cp}(\text{C}_5\text{H}_4\text{CH}_2\text{C}_3\text{H}_4)\text{CpRu}^{\text{IV}}\text{I}]^+\text{I}_3^-$ in which the same electron-exchange reaction is observed as in the case of the salt **1** in solution, although the $\text{Cp}(\text{C}_5\text{H}_4)\text{Ru}^{\text{II}}$ and $[\text{Cp}(\text{C}_5\text{H}_4)\text{Ru}^{\text{IV}}]^+$ moieties are bridged with a nonconjugated $-\text{CH}_2-$ group.³² Therefore a migration of the iodine atom is inevitable for the electron-exchange reaction on **1** and related mixed-valence halobiruthenocenium salts.

In spite of the large temperature dependence of the ^1H - and ^{13}C -NMR spectra of the $[\text{RcRcI}]^+$ cation in a solution, no significant temperature dependence of the ^{13}C -NMR spectra (300–450 K, trapped-valence $\text{Ru}^{\text{II}}\text{Ru}^{\text{IV}}$ type) in the solid was observed for **1** and $[\text{RcRcI}]^+\text{I}_3^-$ on the basis of the results of ^{13}C -CP-MAS NMR spectroscopy in the present study. On the other hand, mixed-valence biferrrocenium salts show a large temperature dependence in ^{57}Fe -Mössbauer spectra.^{8-10,29-31} The reason for the difference is ascribed to different mechanisms for electron transfer; i.e., although electron transfer occurs through the conjugated fulvenide ligand for the latter case, electron transfer takes place through iodine migration for the former; this should result in a larger activation energy for electron transfer in **1** in the solid.

Acknowledgment. We thank H. Oche for the measurement of temperature-dependent CP-MAS ^{13}C -NMR spectra.

Supplementary Material Available: For **1**, tables of experimental data for the X-ray diffraction study (Table S1), atomic positional and thermal parameters for the hydrogen atoms (Table S2), and least-squares planes (Table S3) and ORTEP drawings (Figures S1–S4) (6 pages). Ordering information is given on any current masthead page.

- (28) Abragam, A. *The Principles of Nuclear Magnetism*; Oxford University Press: London, 1961; Chapter 10.
- (29) Nakashima, S.; Nishimori, A.; Masuda, Y.; Sano, H.; Sorai, M. *J. Phys. Chem. Solids* **1991**, *52*, 1169.
- (30) Nakashima, S.; Sano, H. *Hyperfine Interact.* **1990**, *53*, 367. Nakashima, S.; Koura, T.; Katada, M.; Sano, H.; Motoyama, I. *Hyperfine Interact.* **1990**, *53*, 361.
- (31) Dong, T.-Y.; Lin, H.-M. *J. Organomet. Chem.* **1992**, *426*, 369.
- (32) Watanabe, M.; Motoyama, I.; Hano, H. *Inorg. Chim. Acta*, submitted for publication.